Study of the *Resistive Switching* phenomenon in YBCO superconducting samples

by Jordi Antoja Lleonart

Degree in Nanoscience and Nanotechnology, UAB

June, 2014

Directed by Anna Palau Masoliver

Department of Superconducting Materials and Large Scale Nanostructuration, ICMAB

Acknowledgements

First of all, I'd like to thank my director, Dr. Anna Palau, for her time, her patience, her guidance and her help in all the aspects of this project. Regarding the higher echelons of the ICMAB, I am also grateful to Dr. Teresa Puig, who leads the Department of Superconducting Materials and Large Scale Nanostructuration, and the institute's director, Xavier Obradors.

Victor Rouco was in charge of the magnetic decoration procedure, including the SEM imaging, and the sample handling prior to and during transport measurements; not only that, but he also provided very helpful insight during the whole project, as well as analising and discussing the results. I want to show my most sincere gratitude to him and, on the same line, to Ferran Vallés who, after Victor left, helped me out with carrying out and understanding subsequent decorations and transport measurements.

Likewise, at the laboratory level, credit goes to Mariona de Palau, who showed me around at the start of my stay, and who taught me the film pyrolisis and growth procedures, besides being the ceramics laboratory technician. On similar grounds, I thank both Rafael Ortega and Juan Carlos Gonzalez for performing local resistive switching on some of the samples and lecturing me on this technique, and to Bernat Bozzo, who was in charge of the SQUID measurements.

I also acknowledge the help of a miscellaneous group of people who, although not being directly involved with my project, helped me at a moment's notice when I needed it. This includes mostly people from the SMLSN department, such as Cornelia Pop, Pablo Cayado, Victor Rodríguez and Bohores Villarejo.

Finally, thanks to everyone who, in my personal life, was supportive and cheerful. This goes for my family and friends. *Semper Fi!*

Summary

1. Project aims and state of the art

This project seeks to investigate the possibility of using the oxide resistive switching (RS from now on) phenomenon as a means to alter the superconducting yttrium barium copper oxide (shortened to YBCO) in a controlled manner for electronic applications. Current, practical uses of superconductivity are generally in devices where high magnetic fields are required, such as medical magnetic resonance imaging equipment or measuring devices, like SQUID and some PPMS, as will be shown in this project.

Likewise, the use of RS is often associated to the development of novel non-volatile memories, the so-called RRAMs, which could set a new milestone in terms of speed and density of information; however, the ultimate goal of this project would be to further advance in the direction of superconductivity-based, solid state quantum devices, which would in theory have high performance but are so far mainly in a research stage.

Various attempts have been made to tune the properties of superconducting materials in the recent past. These include the generation of artificial pinning centres that are able to improve the performance of a superconductor several times over[i], sometimes controlling this change in a local micrometer scale[ii]; however, none of these techniques provide a reversible way to control the superconducting properties, which would be ideal. In that context, very few research has gone in the way of using RS as a means to reversibly alter the current flow in superconducting materials; there is, however, some evidence that RS can alter the local oxygen doping in YBCO, thus allowing to completelly erase and recover the superconducting state[iii].

Therefore, it is a target of this piece of work to get a first impression of what effects does RS have on the behaviour of superconductors; this will be attempted through magnetic decoration as well as transport measurements using appropriate patterning and optimized metallic contacts. The prime target is to obtain reversible, controllable changes in the superdonducting properties after RS has taken place.

2. Introduction and theoretical basis

2.1. Superconductivity:

This whole project revolves around the phenomenon of superconductivity and superconducting materials. Therefore, it is only fitting to begin by presenting this concept and briefly explaining some of its main properties. What follows is a degree-level condensed introduction to superconductivity, without too much emphasis on mathematical formulism; more on that can be found in the bibliography[iv].

Superconductivity is a physical phenomenon in which the electric resistivity of a certain material decreases to zero below a certain temperature. The resistivity of many metals decreases when temperature gets lower, down to a certain point, but what sets superconductivity apart is that it makes resistivity fall to *zero*. This was observed for the first time in 1911, when Dutch physicist H. Kamerlingh Onnes cooled mercury down to the boiling temperature of liquid helium (4.2 K). The phenomenon that explains this sudden change in the electrical properties of superconductors is the formation of Cooper pairs. These entities come from the coupling of two electrons of opposite spins. The electron pair form due to interactions with vibrations in the lattice of the superconductor, although the exact nature of the pairing interaction in high temperature superconductors is still not clear. This will not be discussed in detail.

Whatever the case, a wide range of superconducting materials has been studied since 1911, each of them with a characteristic Magnetic field-Temperature (H vs T) diagram, as follows.
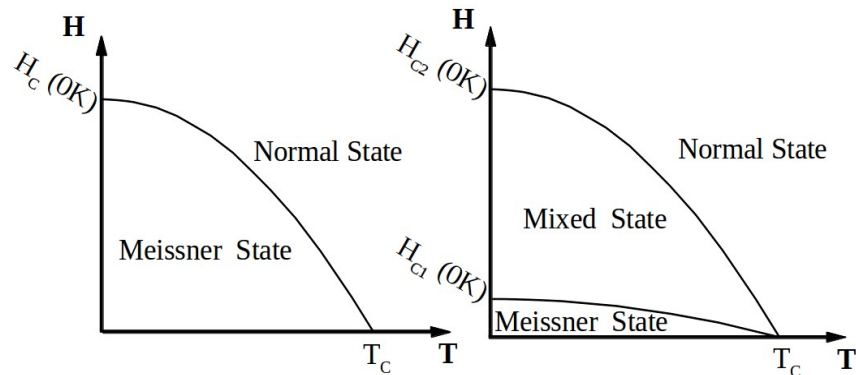

Figure 1: Phase diagram for type I (left) and type II (right) superconductors

At this stage, it is appropriate to introduce the two types of superconductors, namely type I and type II. In type I superconductors, the superconducting state can be reached under threshold, or critical values for temperature (T) and applied magnetic field (H). When these conditions are met, the material is deemed to be a *perfect diamagnet*, which means that its magnetization vector is equal in modulus to the applied field, but points in the opposite way. This effectively means expelling the magnetic field from inside the material, and it is known as Meissner effect.

In particular, in type II superconductors the Meissner effect occurs only as long as the applied magnetic field stays below a certain critical field, H_{C1}, but for higher fields the magnetic flux starts penetrating into the material and the superconductor enters the mixed state. When a value known as *upper critical field* (H_{C2}) is reached, the material becomes normal and superconductivity is lost.

There is still, however, a distinction to be made between type I and type II superconductors. For that matter, two key parameters have to be presented. The first one, λ, is known as the London penetration depth, or more generically just "penetration depth", and it is a measure of how the external magnetic field penetrates in the material. In the easiest case, the field's decay into the superconductor is not a step-like function, but rather a negative exponential, where the external field H_0 has a value of H_0/e at depth λ.

The second parameter, ξ, is not as straightforward to understand. If one pictures the superconductor wavefunction (Ψ) whose modulus squared is the Cooper pair density (n_s), there is also a characteristic depth ξ for the decay of n_s at the boundaries of the superconducting regions. Then, one can work out the ratio $\kappa = \lambda/\xi$ (called the Ginzburg-Landau parameter) for each material. This parameter can be interpreted as how energetically favourable the interface between superconducting and non-superconducting regions are. For $\kappa < 2^{-1/2}$ we have type I superconductors, where the interface is minimized, that is, the boundary between states is theoretically placed at the material's boundaries (the whole body is superconducting); when $\kappa > 2^{-1/2}$ the material is a type II superconductor, and interfaces are favoured. When this happens, a new mixed state appears beyond the Meissner state, where magnetic field penetrates inside the material forming quantized magnetic flux lines (with non-superconducting materials in their

core), called vortices.

The magnetic flux in each vortex is a constant, called the *flux quantum* or *fluxoid, Φ_0;* therefore, in the mixed state (which is where vortices are present), an increase in the applied magnetic field causes an increase in the *density* of vortices rather than in the magnetic flux through any one of them.

$$\Phi_0 = \frac{h}{2e} \approx 2.07 \cdot 10^{-15} T \cdot m^2$$

The presence of a vortex in a superconductor implies that there is an electrical current running around it, much like the current through a coil generates a magnetic field inside it. In the case of a vortex, however, these currents take place in the superconducting region i.e. they face close to zero resistivity. On the other hand, the region inside the vortex is *not* superconducting; therefore, any movement of the vortex will involve movement of non-Cooper-paired electrons and eventually lead to scattering and thermal losses.

Vortices in a clean superconductor are distributed evenly in a hexagonal lattice, but this is generally true only for a perfect monocrystal, as shown in the previous figure. Wherever there are lattice defects, these tend to not be a part of the superconducting region, and so vortices may be anchored there, losing their hexagonal symmetry. This will be explained in more detail further ahead, but the main point is that when vortices *are* pinned in defects, there are interesting phenomena going on. On the one hand, if a current is applied across the material, a Lorentz force is exerted upon the vortices, generating their motion and thus Joule effect related losses. On the other, defects able to anchor vortices may be used to generate a *pinning* force that prevents this motion and allows loss-free electrical transport in presence of a magnetic field. In this context, if the losses associated to vortex movement can be eliminated, their use in highly efficient current transport could be feasible in practice.

The maximum critical current that can be applied to a superconductor without vortex motion (i.e. dissipation) is ruled by two forces; the pinning force, which is dictated by the nature and number of defects in the solid, and the Lorentz force, which scales with the applied magnetic field and current density, as:

$$\vec{F}_L = \vec{J} \times \vec{B}$$

Pinning will only occur whenever the pinning force is higher in value than the Lorentz force, and so there will exist a certain critical field over which the vortices are free to move. This field varies with temperature, and together they form the so-called *irreversibility line* that separates the solid vortex lattice, to the left, and the vortex liquid to the right. To put it in another way, when this line is crossed to the right, the critical current density, J_C (maximum current density that can be achieved without dissipation) becomes zero.
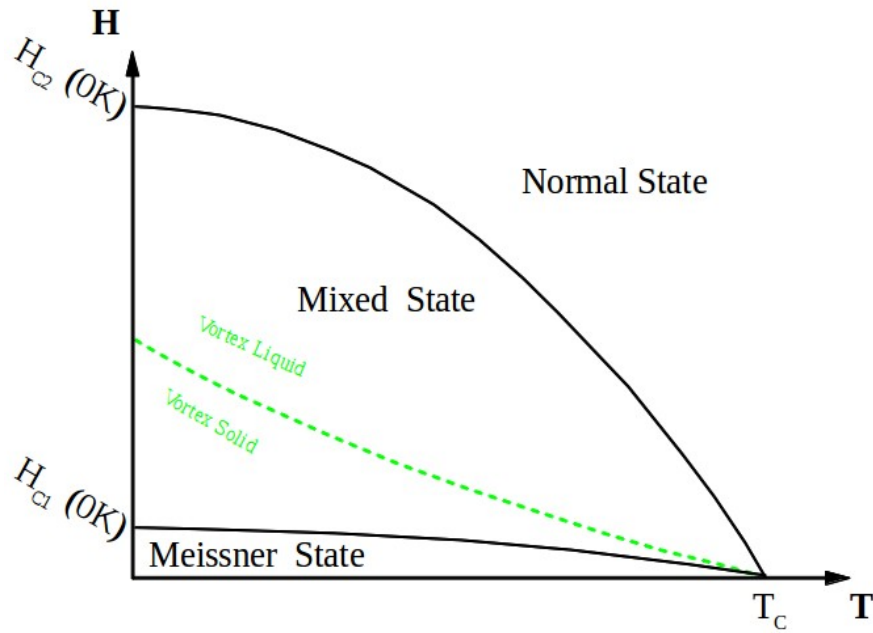

Figure 2: Simplified phase diagram for type II superconductors. Note that the irreversibility line (green dashes) meets the other two at H=0

This project seeks to exploit the possibility to generate artificial vortex pinning in *high-temperature superconductors* (HTS) by using the resistive switching effect (described in the next section). The HTS term is generally used to refer to materials with critical temperatures over nitrogen's boiling temperature (77 K). They are technologically relevant because their use does not specifically require cooling processes that use liquid helium (which is, of course, much more expensive than liquid nitrogen).

The material of choice for that matter was, due to its high (in H_C) irreversibility line, $YBa_2Cu_3O_{7-X}$ (X lower than 1), as mentioned previously. It is a high-temperature superconductor with critical temperature around 93 K in bulk form, and slightly lower for thin films. It has a perovskite structure as shown in the figure; it is formed by a stack of Cu-O planes lying normal to the c direction. These planes contain mobile charge carriers and they are where the supercurrent flows; they are separated by charge-reservoir interlayed layers which allow changes in the carrier density available in the Cu-O planes. The magnetic fields applied in this project will follow the c (vertical) direction and the transport current will be applied along the Cu-O planes.

Y

Ba

Cu

O
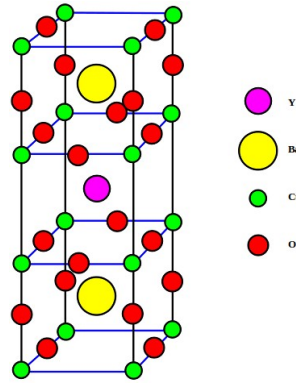
Figure 3: YBCO crystal structure; the blue lines indicate the Cu-O planes.

2.2   Resistive switching:

The RS phenomenon plays an important role in this project, and for that reason, it will be briefly explained. This phenomenon involves inducing two reversible resistance states (ON/OFF) in a material upon the application of an electric field. The possibility to use the resistive switching effect to generate low-resistance (non-superconducting) regions in the material would open the possibility to create reconfigurable pinning centres in the superconductor, which would be very useful for applications based on fluxtronics (manipulation of flux quanta).
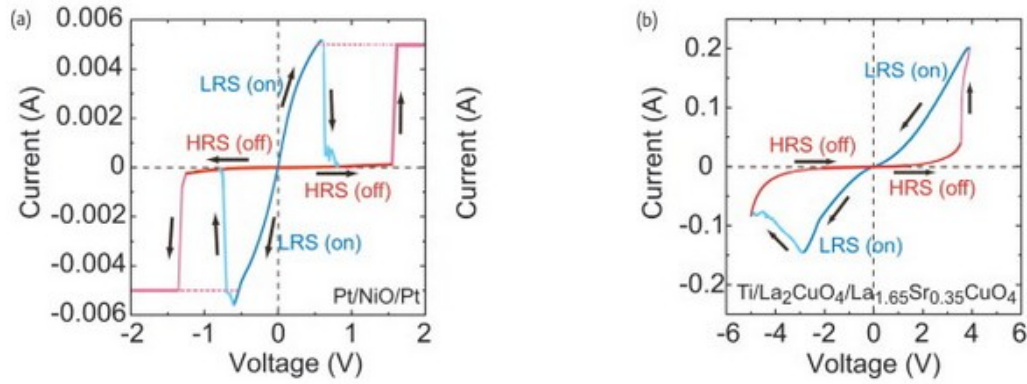
9

Figure 4: a) Unipolar RS: the change from the Low-Resistance State to the High-Resistance State, and vice versa can happen at voltages of the same sign. b) Bipolar RS: the change between states happens only at voltages of opposite sign. (Source: reference V)

There are several models to explain this resistance change depending on the material[v], from the reversible formation of conducting filaments to the generation of charged interfaces along the voltage difference. The exact nature of the change in complex oxides like YBCO is still not agreed upon, but evidence points at the generation of oxygen vacancies as one of the possible causes. In any case, it is generally accepted that this switching has a very low penetration depth, and therefore the use of thin superconducting films will be a necessity if substantial changes in their transport properties are to be observed.

3. Experimental Procedures

3.1.   Sample Preparation:

Let us not forget that the main objective of this project is to study the resistive switching effect in YBCO thin films. As mentioned in the introduction, these films are highly anisotropic and thus they must be epitaxially grown in order to obtain good superconducting performances. To do so, we will use the chemical solution deposition (CSD) method, which is a very promising route to obtain long superconducting wires that could see large scale application. This method has many variables that must be optimized to obatin high quality superconducting YBCO films. This chapter will detail the CSD process used to grow the studied samples, which is based on the use of metal trifluoroacetates; this is the TFA route, first displayed in the late eigthties.

To begin the process, one needs an adequate precursor solution. This had already been done by the start of the project, therefore it will not be explained extensively. The main line involves using either YBCO powder or the hydrated trifluoroacetates of Y, Ba and Cu; either way, after some heat treatment, the salts would be dissolved (this could take around 48 h at 50ºC) in a mixture of acetone and trifluoroacetic acid, and placed in vacuum for the solvents to evaporate. The leftover solid, still containing the metal salts, can be redissolved in ethanol or methanol in order to yield the precursor solution, which is dark green in colour.

For this project, that solution was diluted at a 1:4 ratio in methanol. This ultimately leads to the final films being substantially thinner than those obtained with the standard solution (of 250 nm), down to about 50 nm in thickness. The substrate of choice was monocrystalline LAO (Lanthanum aluminate, $LaAlO_3$), which is diamagnetic and has a lattice constant of 3.905 Å, similar to that of YBCO, 3.88 Å (0.64% mismatch). The substrates, with sizes 5mmx5mmx0.5mm, were one-side polished and had been previously treated via an annealing in presence of oxygen, and cleaned with acetone and methanol afterwards in order to start with a clean surface.

Each substrate was spin-coated with 15 µl of the diluted YBCO solution inside a dry

box/chamber at 6000 rpm for 2 minutes. After roughly five minutes on a 70ºC hot plate, the samples were placed in a tubular furnace, starting the pyrolisis step. This process ramps the sample up to about 300ºC under a constant oxygen flow; a certain level of humidity is added via a water bubbler above 100ºC so as to prevent the sublimation of copper trifluoroacetate.

After this step, the thin film usually has a blue colour, which may vary from green to purple depending on the thickness. Some defects may be visible near the edges at this stage, since it is where the initial coating was thicker; in some cases, one can observe cracking and buckling of the pyrolized film (caused by quick shrinking upon heating). It is almost guaranteed that these defects will damage the final superconducting properties, so some samples may be discarded at this point.

The final process is YBCO growth and, since it also involves the use of a furnace, it may be performed right after pyrolisis. The sample is heated to roughly 800ºC in a mixed O_2 and N_2 flow, as well as an initial water vapour flow. At the end of this step (which in this case takes place overnight) the sample can be retrieved, and it normally has a golden glowing look, although the sample edges and defects can sometimes retain their blue colour, indicating regions of poor epitaxial quality.

At this point, the thin film is finally a heteroepitaxial YBCO 50 nm film. Care must be taken to store it in dry conditions, as room humidity can damage the surface layer and render it useless for any superconductivity-related purposes in a matter of hours. Before the following procedures, the quality of the samples is assessed by SQUID (Superconducting Quantum Interference Device) measurements, which in this case were used to determine, among others, their critical current density at 5 K and 77 K and their critical temperature. The films with the best superconducting performance were used for this project. Below are the results of some of these measurements.
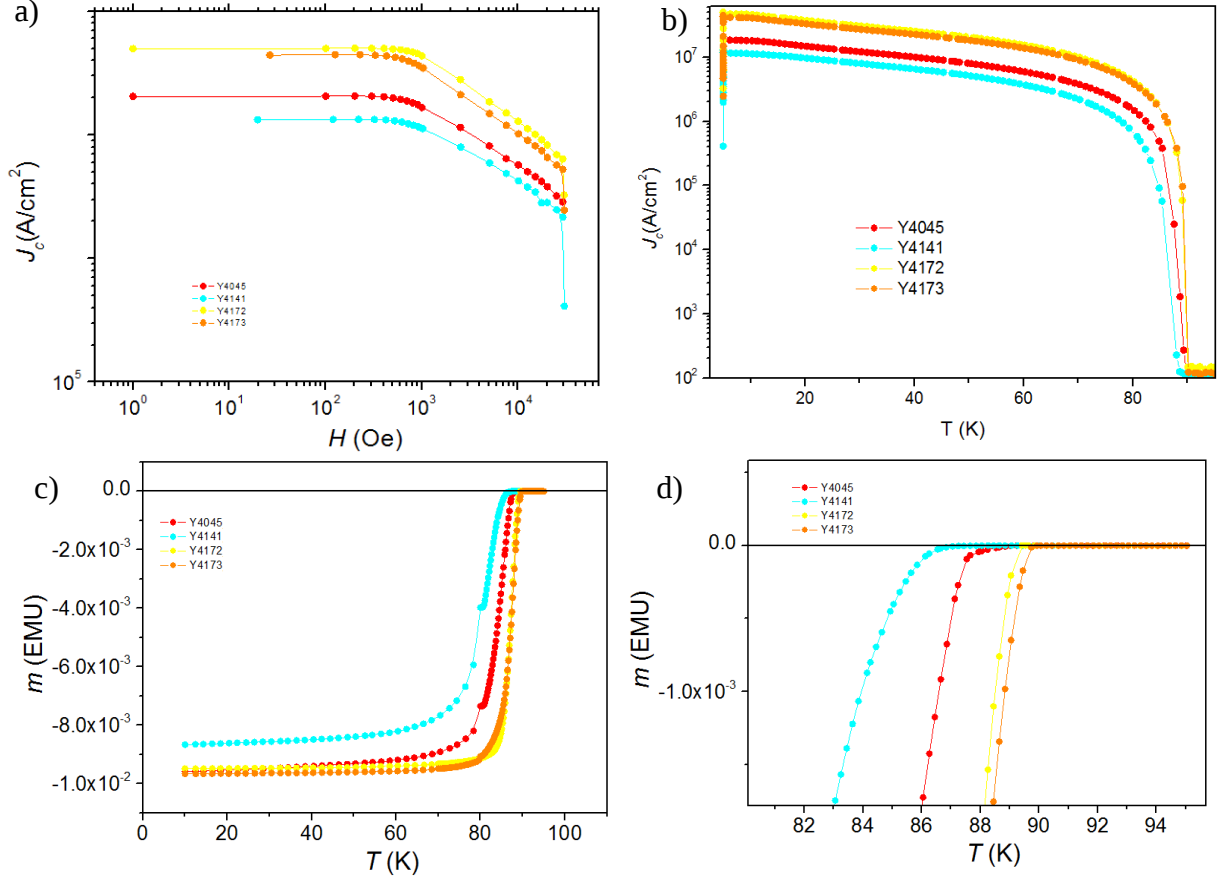
Figure 5: SQUID measured curves for four of the best samples: critical current versus applied magnetic field (a) or temperature (b) and magnetization versus temperature (c and d).

3.2. Bitter decoration:

The primary characterization technique that we chose to study the effect of resistive switching on vortex pinning was the Bitter decoration technique, also known simply as magnetic decoration. The local changes in the material properties caused by oxide RS should have some effects in the vortex lattice pinning, and a way of checking this is monitoring the magnetic vortices' positions by magnetic decoration.

Magnetic decoration is a technique in which a small superconducting sample is placed inside a vacuum chamber with a controlled helium pressure and applied magnetic field. In front of it, a tungsten wire with an iron source is positioned so that, by resistive heating, iron particles can be

emitted. Depending on the He pressure, these particles suffer a number of scattering events, and eventually they may collide and form larger aggregates with a substantial magnetic moment.

If this experiment is performed at sufficiently low temperature (generally in a liquid helium bath) and a high enough applied magnetic field, the magnetic vortices that will be present in the sample will interact with these aggregates, whereas the superconducting parts will not. In the end, the evaporated iron will end up mostly on top of each vortex, stuck in place via van der Waals interactions, and it will stay there even after room pressure and temperature are restored.

After this process, the decorated samples may be observed by Scanning Electron Microscopy (SEM). However, due to the fact that these observations are performed at room temperature and that YBCO is not a very good conductor at this stage, care must be taken to place a good amount of copper film around the sample borders, to avoid to some extent charge build-up at the surface of the film, which would eventually lead to poor imaging.

3.3.   Resistive switching:

In general terms, the electric field that is required to switch the material is applied via two conducting tips. If an AFM (Atomic Force Microscope) is used for this purpose, the mass is connected to the outer rim of the sample, whereas the tip at the end of the cantilever is the one with applied voltage. In this project, however, the most used approach was to work with a probe station, which could fit up to four Au/W alloy tips. This approach is not as precise, mainly because all the alignments are performed with an optical microscope rather than the AFM imaging, but it allows for quick and straightforward measurements.

The RS measurements are voltage sweeps between the two terminals where the electric current is registered; the limit of detection is roughly 1 pA. One of the terminals is defined as negative (mass) and the other as positive (applied voltage); in theory, the changes in the material happen mostly near the positive terminal. Generally speaking, the sweeps are between 0 V and a defined value, which in this project was never larger than ±10 V. A current ceiling (compliance) also needs to be set; the chosen value for this parameter was 0.1 A.

3.4.   Transport measurements:

If the local superconducivity of the sample needs to be assessed, one of the most direct kind of measurements is to measure its electric transport properties. For that matter, some of the superconducting samples were patterned defining current tracks of known size.

The first step after obtaining a sample (Y4141) with good superconducting properties (checked by SQUID measurements) was the thermal evaporation of gold to achieve a number of contacts, which could be later used both for attaching the equipment wiring and for acting upon the sample. Knowing the design of the final circuitry, three large square pads were placed in the middle, with eight smaller contacts in the borders.

After these were achieved, the actual optical lithography could begin in the 10000-class clean room. The computer-generated mask was based on a previous design, with four tracks, each ready for Four-Terminal current sensing. For this project, however, the tracks were thinned to about 20 µm in width and 50 µm in length, leading to a cross-section of about 10^{-12} m^2 or 10^{-8} cm^2, assuming that the film's thickness remained constant throughout the process.
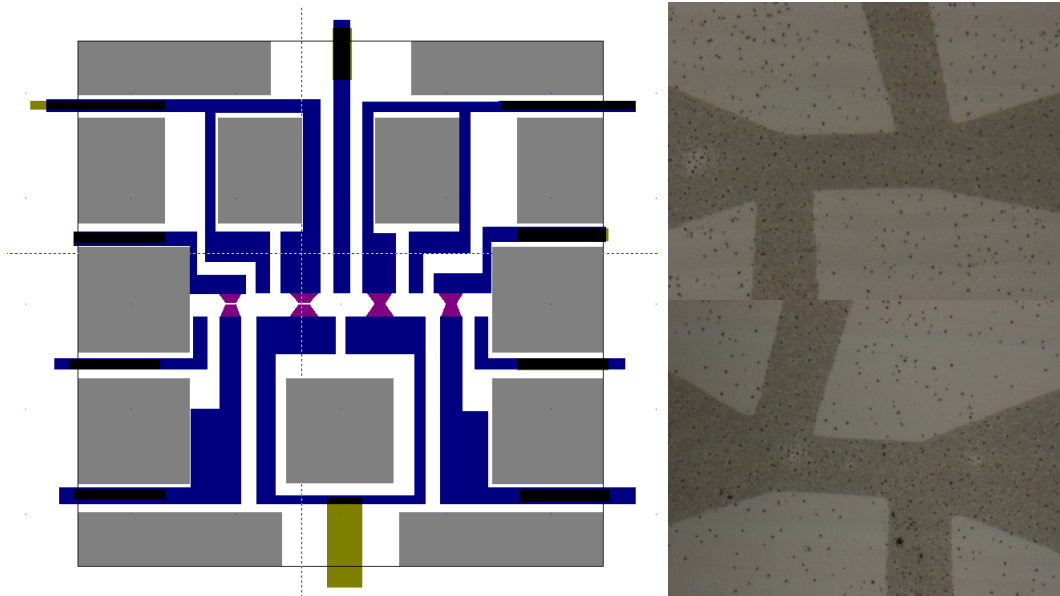

Figure 6: On the left side, base mask design for four terminal measurements. The white regions are where YBCO will remain untouched, whereas it will be etched away in the blue and purple areas. The grey rectangles mark the position of the metal pads. Notice the narrow tracks, 1 to 4 (left to right) between the purple polygons. On the right side, Optical transmission microscope images of Track 1 (top) and Track 4 (bottom) after the etching took place. In light grey, LAO substrate and in dark grey, remaining YBCO.

After the mask design was over and the sample had been spin-coated with the positive photoresist, the optical LASER lithography began (using a Durkham Magneto Optics LTD Micro-Writer). After the sample had been developed, it was taken out of the clean room, etched with 1:1000 phosphoric acid and cleaned with acetone afterwards. Any short-circuits that could have arisen between the gold contacts were carefully removed with 1:10 phosphoric acid as well.

After the patterning, the sample was subsequently placed in a clean puck (pictured below) which was compatible with the Physical Property Measurement System (PPMS from now on), stuck to it with double-sided copper tape and surrounded in heat-conducting grease. Afterwards, it went *back* to the clean room, this time to use a wire bonder (Kuliche & Soffa Wire Bonder 4526) to contact two of the tracks, T1 and T4, to the puck's metal pads; up to three or four aluminum wires were used for each contact, owing to the fact that some of them might eventually detach from either surface.

At this point, a multimeter test showed that the resistance of either track was of the order of 1 or 10 kΩ. This is consistent with the known track sizes; for a room temperature resistivity of approximately 0.008 Ω·cm [vi], the expected resistance would be around 4 kΩ; this is taking only the tracks themselves into account and disregarding all the rest of the circuit. With the knowledge that the contacts seem to work fine, the sample was taken to the PPMS and placed inside the helium-cooled chamber; after the routine calibrations, the measurements of T1 and T4 could be performed. The sample was zero-field-cooled down to 60 K from room temperature whilst the two tracks' resistances were being measured, and afterwards their critical currents were obtained at 60 K for magnetic fields up to several Tesla.
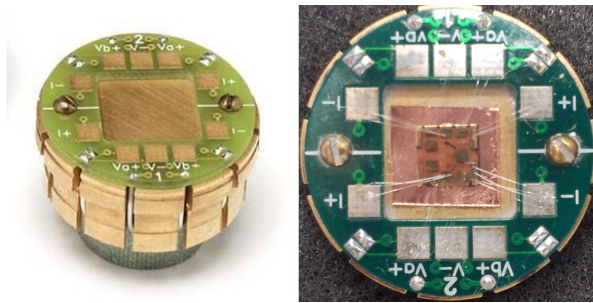

Figure 7: PPMS puck, both empty (left; source: QD China) and with a 25 mm^2 sample stuck and contacted (right).

4. Results and Discussion

4.1. Bitter decoration:

For the first decoration attempts, two PLD-grown (Pulsed Laser Deposition) samples were used, owing to their higher surface quality. By doing so, we wanted to assess the actual chance of success using the cheaper CSD-grown films, which usually show some precipitates at the surface that could complicate the vortex identifiation. The PLD samples were field-cooled under 33 Oersted, and decorated in 170 mtorr He. The first images are from a 150-200 nm film:
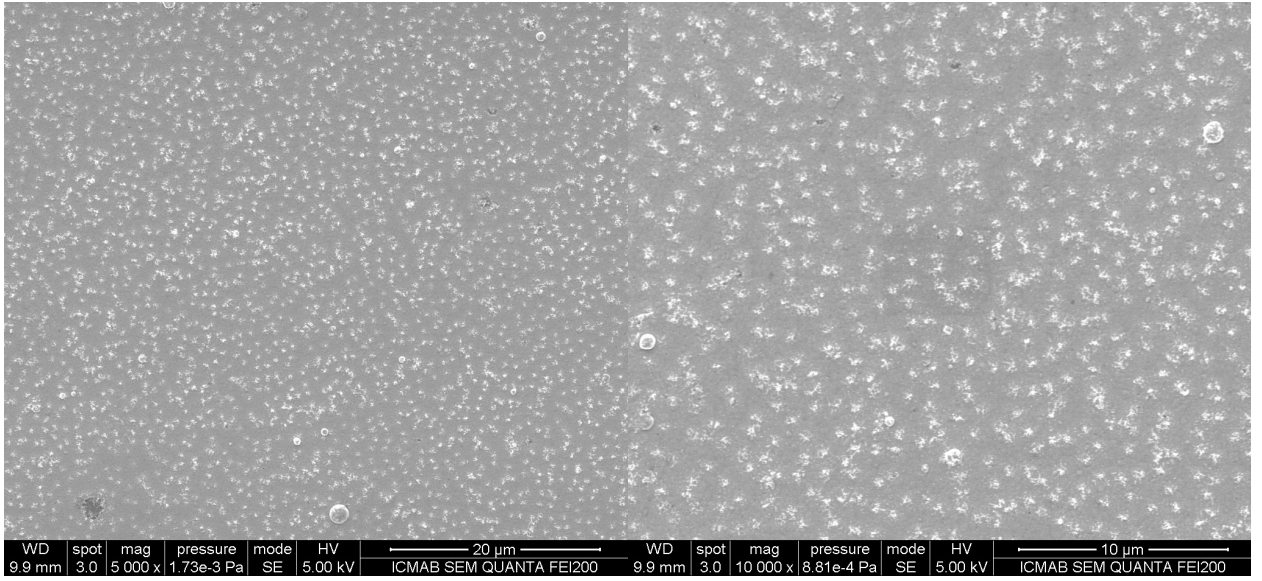
Figure 8: SEM secondary electron images of different regions of sample S15. The YBCO film is seen as a grey background, and the iron aggregates are the small white shapes; some larger droplets can also be seen.

Now, if one assumes that the vortices were perfectly still when the iron landed on them, a hexagonal lattice should be expected. However, there are a variety of defects in the film, both isotropic and anisotropic, which act as pinning centres and result in a seemingly random pattern, as seen above. Given that these results are satisfying, the following step is to perform another decoration in a thinner sample.

It should be taken into account that the RS phenomenon is localized near the sample surface and thus thinner samples must be investigated in order to be able to observe the effect of RS in

vortex pinning. For this, a PLD YBCO film of 50nm in thickness, underwent the same decoration procedure, and the result was not so satisfactory:
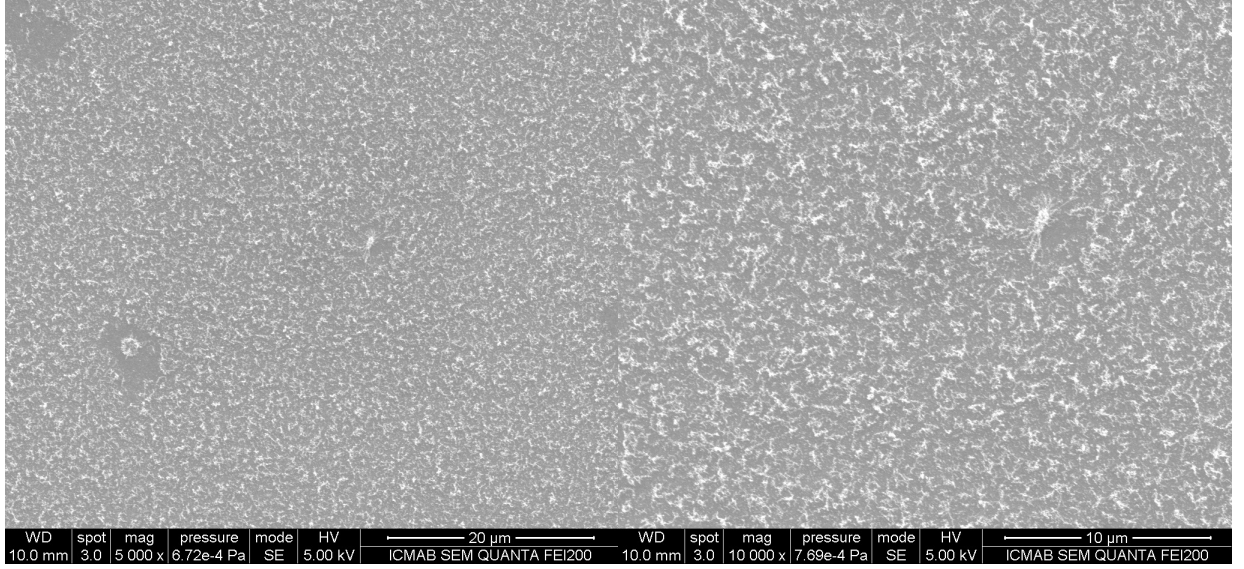

Figure 9: SEM secondary electron images of different regions of S20.

The vortex locations are not so easily determined in this case. This is due to the lower thickness of this film, and it can be roughly explained by the spreading of the vortices depending on the size of our material. Whenever we are not dealing with bulk materials but thin films, a new penetration depth for the magnetic field, Λ, is used instead of λ.

$$\Lambda = \frac{\lambda^2}{t}$$

The fact that it is proportional to t^{-1} (t being the material's thickness) means that, for very thin films, the penetration depth will be larger. If this happens, the magnetic field goes through the sample in a wider area around each vortex, as shown in the following figure, which would allow the iron aggregates to land in less discrete locations.
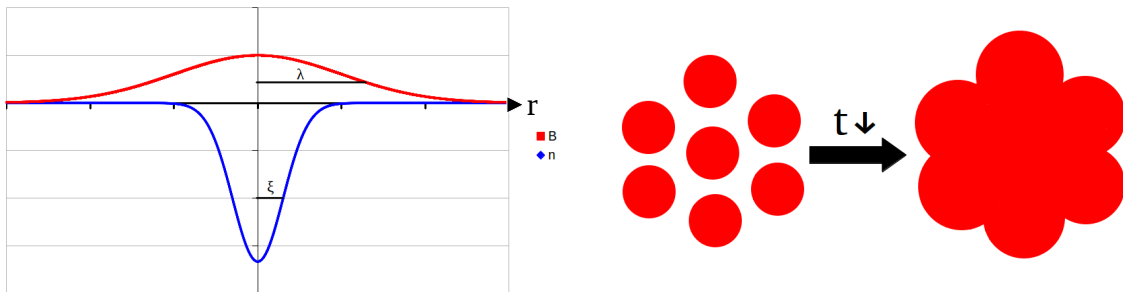

Figure 10: On the left side, qualitative schematic of the magnetic field and the supercarrier density near a vortex. On the right side, sketch of the magnetic field penetration in a vortex lattice upon film thickness reduction.

As interesting as it may be, this phenomenon poses a serious threat to the feasibility of the decoration experiments on CSD-grown films of 50nm. Their thickness is the same as that of the thinner PLD sample, and their surface quality is likely not as good; therefore, we have concluded that the decoration technique was not a useful tool to evaluate the RS effect in YBCO thin films.

4.2.   Resistive switching (I-V curves):

The next step before the optical lythography could take place was to determine what the optimal contact material was to perform the RS experiments. Metal contacts are a requirement if the probe station approach is used as opposed to the AFM, as they can greatly reduce the contact resistance that would otherwise arise between the tips and the oxide and assure a better reproducibility. According to our measurements (shown further ahead), the use of contacts can result in a current increase of about two orders of magnitude versus the same sweeps performed directly on YBCO. For this project, silver and gold contacts were compared; in both cases, 50 nm-thick squares were thermally evaporated on two of the CSD-grown samples. Due to the low thickness of the films, they were *not* annealed afterwards, which is useful to improve contact adherence but can also generate some diffusion of the metal in the sample.
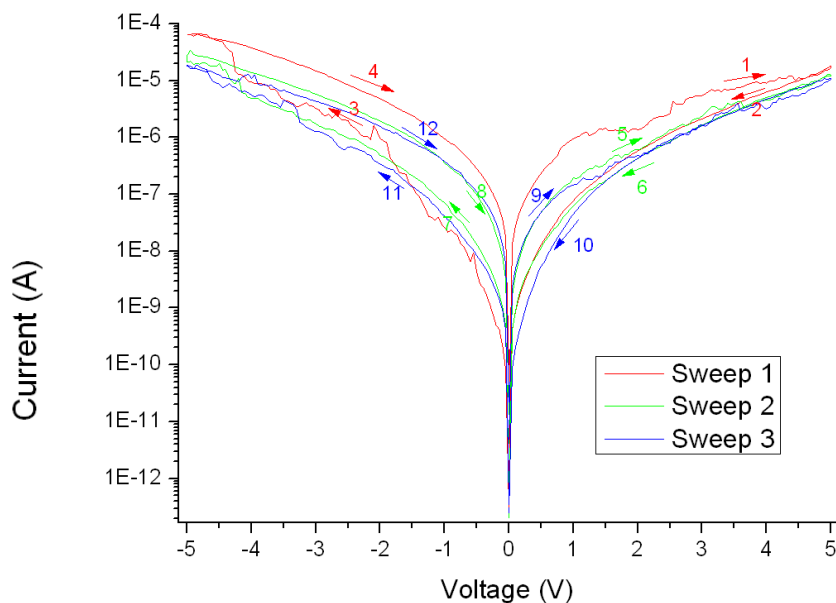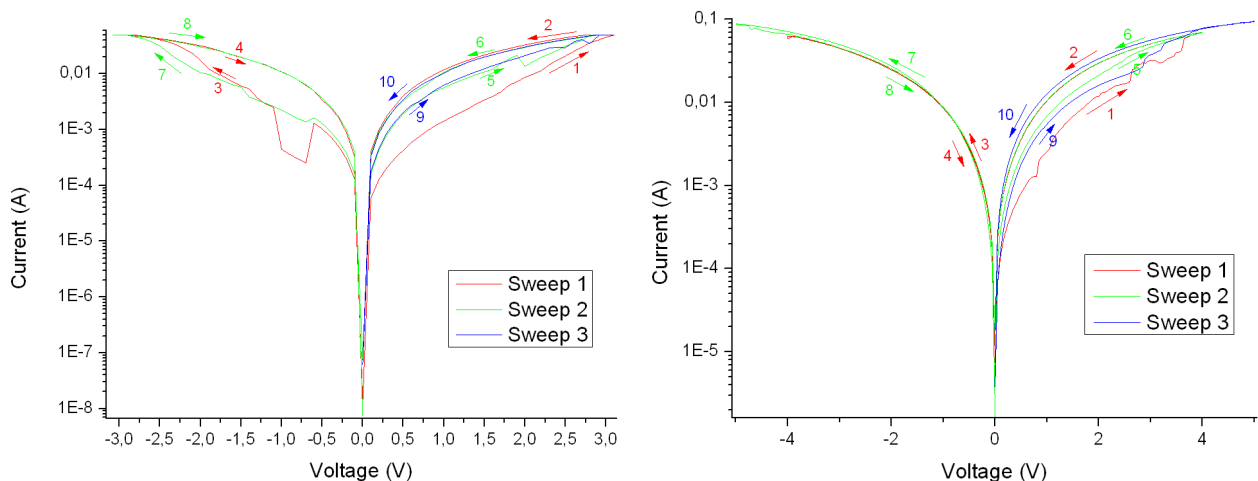

Figure 11: I/V curve for Y4173 with both tips on bare YBCO.

It would also be desirable that the contacts provide non-volatile RS. This refers to the fact that the resistance states must be conserved from one switch to the next. The figure above, where no contacts were used, is a good example of non-volatile switching; it can be seen that, for instance, sweep 2 ends in a low-resistance state (8) and sweep 3 starts in a LRS as well (9). If the switching is volatile, any changes that are made in the conducting tracks are not guaranteed to be still in effect when the transport measurements are carried out.

Figure 12: I/V curves for Y4172 (Ag contacts, left) and Y4173 (Au contacts, right) with both tips on the metal contacts.

In this regard, it was found that silver was not as good as gold at keeping the resistance state of the material. Measurements performed with the two conducting tips over the contacts showed some differences between the different sweeps performed on either sample. In most of the cases, we observed volatile RS when using silver contacts (Figure 12, left), while non-volatile RS was obtained with gold contacts (Figure 12, right).

However, when one tip was placed on a contact and the other was contacted directly to the YBCO film, the sample with the silver contacts sometimes swapped resistance states between consecutive sweeps; other times, the resistance state was conserved. Under the same conditions, the golden contacts allowed up to ten sweeps with mostly consistent (non-volatile) switching before the material broke down.
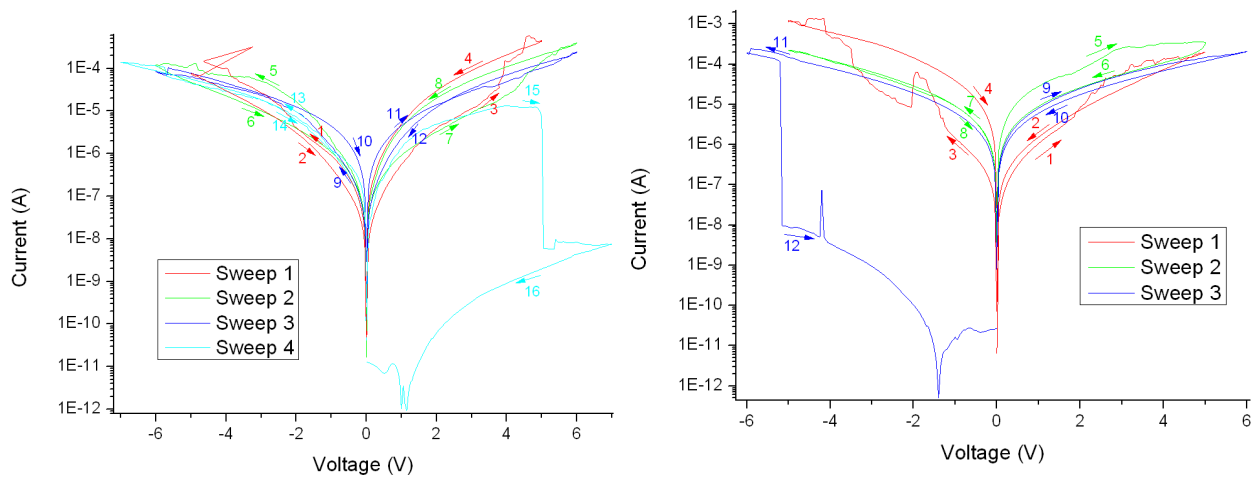
Figure 13: I/V curves for Y4172 with the positive (left) or negative (right) tip on a Ag contact.

The effect of the polarity of the contacts was also tested for each sample. Although the results were admittedly not very reproducible, the material's response seemed to be less volatile when the positive tip was placed on the contact than when the negative one was there. The order in which the sweeps were performed (positive first or negative first) was varied but no clear tendency was observed in the results.
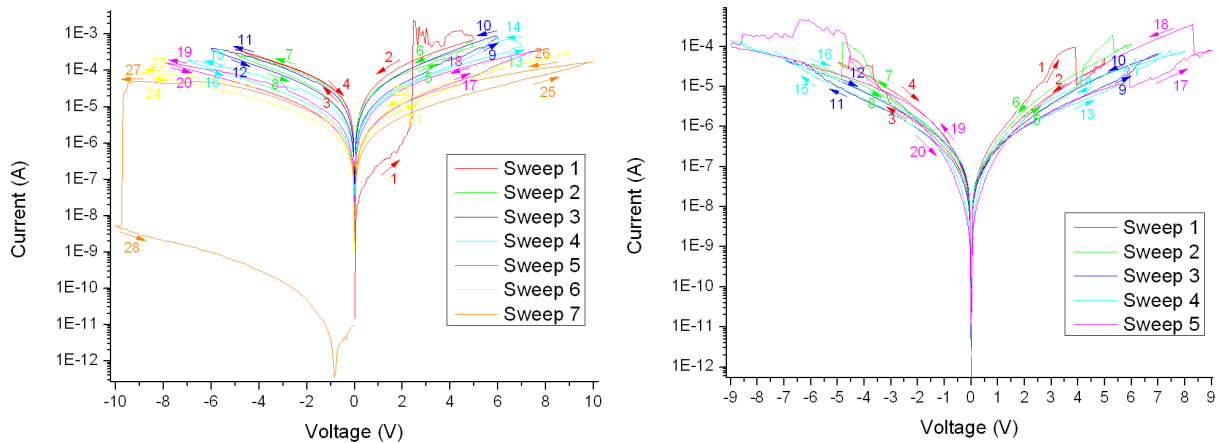

Figure 14: I/V curves for Y4173 with the positive (left) or negative (right) tip on a Au contact.

Taking all the results gathered into consideration, it seems that the optimal way to perform RS on the tracks and witness its effects afterwards is to use gold contacts. Ideally, both tips should be placed on gold contacts so as to maximize the electric current, but this would require to also evaporate a layer of gold on top of the track, and was out of the scope of this project.

4.3.   Transport measurements:

The following curves were obtained for the patterned YBCO sample by means of transport measurements.
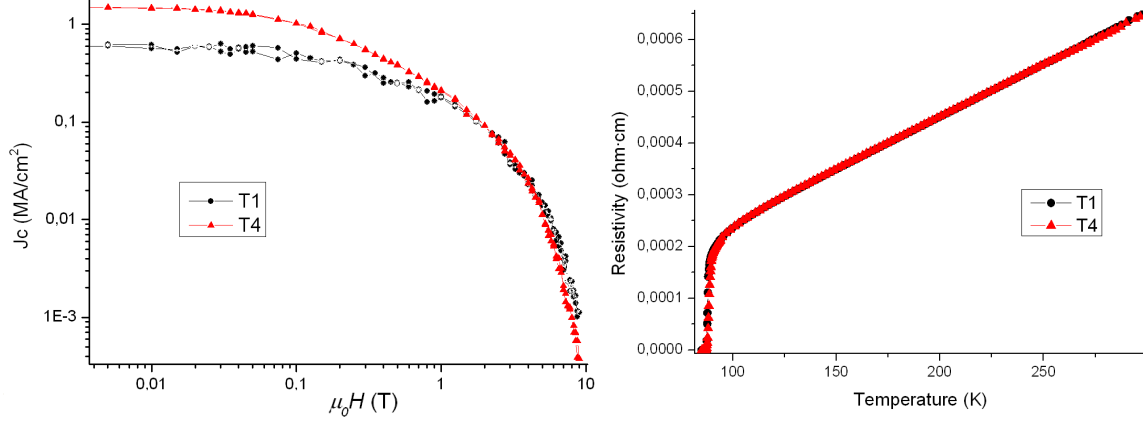

Figure 15: PPMS-obtained J_C vs H (at 65 K) and ρ vs T plots for Y4141. In these measurements, T_C was found to be between 87 and 88 K for both tracks.

From these measurements, it was observed that the critical temperature obtained was lower than that in the bulk material, as already shown in the characterization measurements performed by SQUID. Moreover, the values of J_C were not the best for a YBCO film either. Although much better samples were obtained during the course of this project, we used this one for transport characterization since this procedure requires a lot of steps of preparation that must be performed at the beginning of the project. The better samples, with higher J_C, were achieved after several growth trials and could not be used for this purpose.

Now, our objective is to use transport measurements to analyse the superconducting properties of a YBCO track before and after the RS effect. With this approach the effects of oxide RS can be evaluated in a way that did not require the sample to be thick and smooth as is the case for Bitter decoration.

Once the transport characteristic curves have been obtained for the pristine tracks, they were exposed to an electric field via the probe station, as previously described. After some tests run on a different, blank YBCO thin film (Y4172), it was apparent that the voltage required to switch to the high-resistance state was below 10V. Below are the graphs showing the I/V sweeps
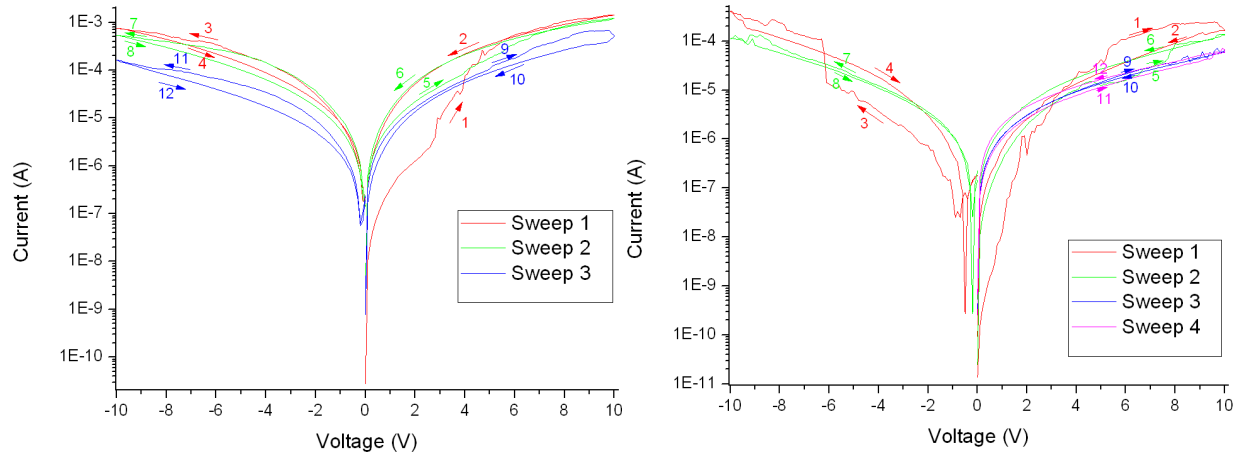
performed on two different tracks, T1 and T4.

Figure 16: I/V curves for the first RS of T1 (left) and T4 (right).

As shown in the graphs, both curves start with a forming stage (1), and after some sweeps both tracks were taken to the high-resistance state (HRS). A certain discontinuity is observed in the resistance state for various loops (i.e. for T4, Sweep 2 ends in the HRS but Sweep 3 starts in the LRS), hinting at some volatility in the oxide. Nevertheless, Y4141 was taken back to the PPMS to measure its superconducting properties after the RS procedure (results shown further ahead).
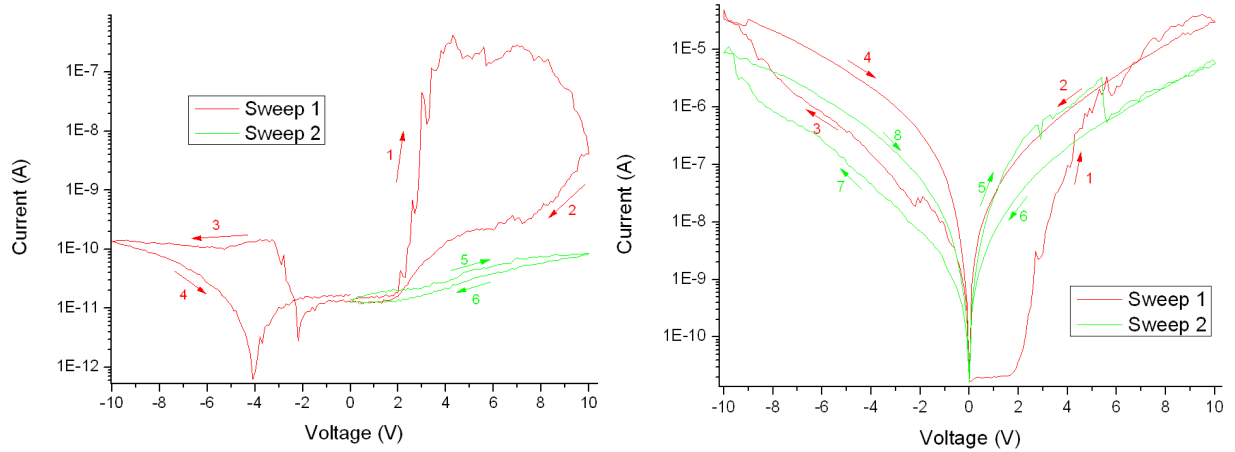

Figure 17: I/V curves for the second RS of T1 (left) and T4 (right).

Afterwards, a second round of RS was carried out again on T1 and T4. This time, an attempt was made to leave the samples at their LRS. Although it was seemingly achieved with T4, the results of T1 were not as good, as it seemed that some sort of breakdown had happened after several a couple sweeps. The sample was taken to the PPMS one last time to measure the transport properties of the bridges.
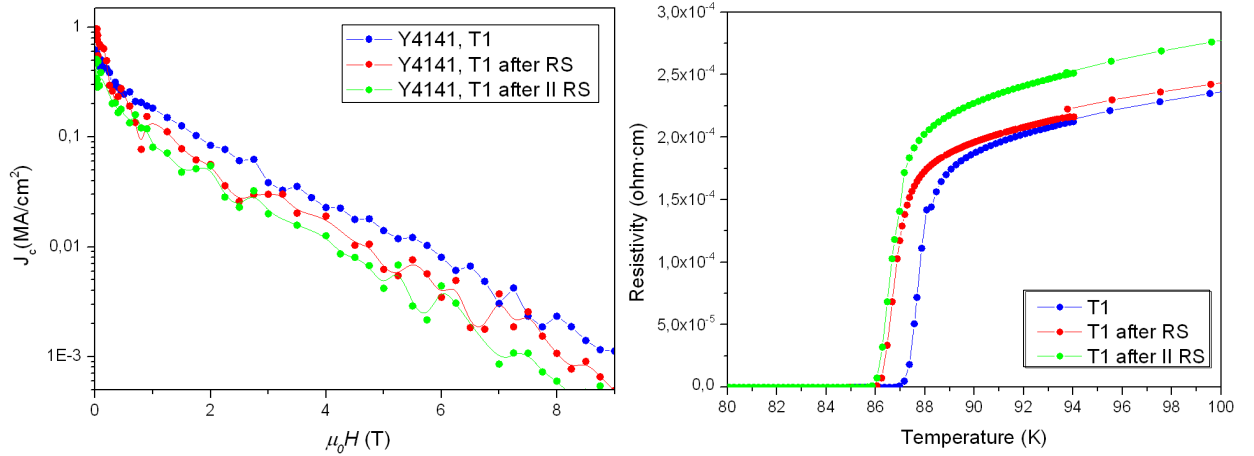
Figure 18: J_C vs μ_0H (left, 65 K) and ρ vs T (right) for T1 at the three stages of RS.

For Track 1, the first RS step caused a slight decrease in current density, as well as a roughly 1 K drop in critical temperature. When the second RS step was carried out, the current density decreased again, and the critical temperature remained essentially the same. This suggests that, indeed, T1 was not brought to the LRS after the second round of RS but degraded to some extent instead.
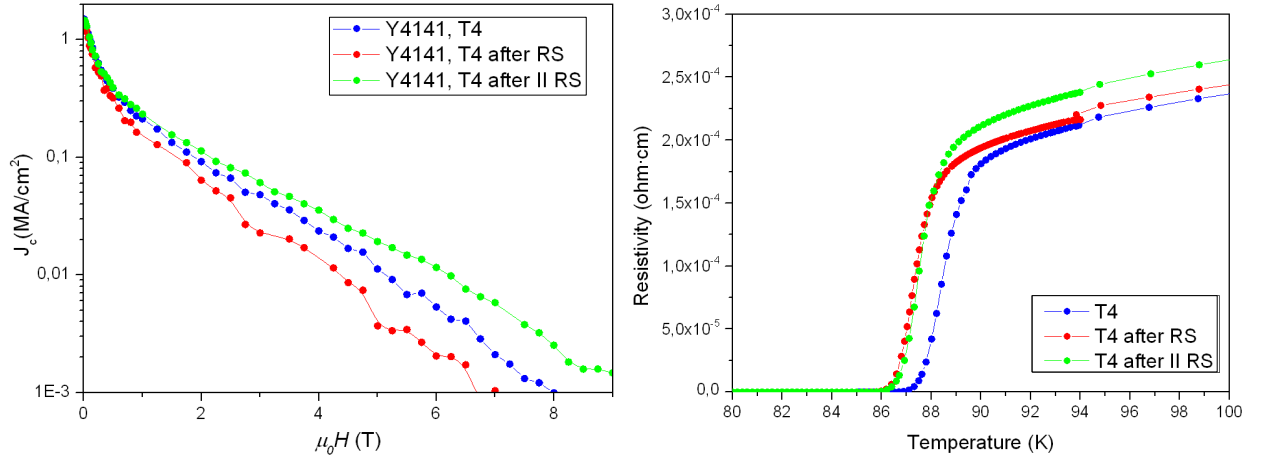

Figure 19: J_C vs μ_0H (left, 65 K) and ρ vs T (right) for T4 at the three stages of RS.

The results for T4 are more in line with the initial target of this project. It is clear from the first graph that the current density decreases with the first RS step, as intended, and increases again with the second RS step, which indicates that the track was successfully brought back to a conducting state. The T_C has been slightly recovered throughout the second RS, but the resistivity has not. So, we can conclude that we have been able to modify the transport properties of YBCO in a reversible way by using the RS effect.

5. Conclusions

In this project, the CSD method was proven as a way to obtain cheap, reproducible thin films with very high superconducting performance (J_C of several MA/cm^2 at 77 K) provided that the process conditions were adequate. The Bitter decoration technique, although a useful complement to the main line of this project, could not be used to successfully visualize the effect of RS on the vortices of these superconducting films.

The evaporation and testing of different types of metal contacts provided useful information if attempts at RS are taken in the future with similar samples. It became apparent that gold contacts are generally better than silver in this case, although it is possible that other materials, such as platinum, should be also considered in this regard.

All things considered, it is clear that the superconducting properties of the sample have been altered to a certain degree upon RS, and it is likely that these changes are due to a change in the oxygen doping of the superconducting film. However, these changes are not fully controlled and a less crude approach will be needed for more reproducible results. This would include, as aforementioned, trying to cover the tracks with gold, but also, and perhaps most important, to find a proper way to align the tip so that subsequent RS steps all take place in the same spot.

Anyhow, we have been able to successfully produce reversible switching effects in YBCO bridges, which indicates that resistive switching seems to be a promising way to reliably and reversibly change the resistance state of YBCO. Further study in this field could one day lead to a new generation of solid state reconfigurable electronic devices if the hassles found within this project can be overcome.

References

i   Kaname Matsumoto and Paolo Mele, *Artificial pinning center technology to enhance vortex pinning in YBCO coated conductors,* Superconductor Science and Technology, Volume 3, Issue 1, 014001, December 2009.

ii   Katzer et al., *Gold nanocrystals in high-temperature superconducting films: creation of pinning patterns of choice,* New Journal of Physics, Volume 15, Issue 11, 113029, November 2013.

iii   Tulina et al., *Oxygen doping of HTSC and resistive switching in HTSC-based heterostructures,* SpringerPlus, Volume 2, 384, August 2013.

iv   Cullity, B.D. And Graham C.D. 2009, *Introduction to magnetic materials,* Second Edition, IEEE Press, Piscataway (NJ).

v   Akihito Sawa, *Resistive switching in transition metal oxides .* Materials Today, Volume 11, Issue 6, p. 28-36, June 2008,

vi   Banani Parida, *DC Electrical Resistivity Studies in bulk YBCO/Ag composites.* National Institute of Technology, Rourkela, India, 2011.

Acronym index

AFM: Atomic Force Microscope

CSD: Chemical Solution Deposition

HRS: High-Resistance State

HTS: High-Temperature Superconductor

LAO: Lanthanum Aluminate

LRS: Low-Resistance State

PLD: Pulsed Laser Deposition

PPMS: Physical Property Measurement System

RS: Resistive Switching

SEM: Scanning Electron Microscope

SQUID: Superconducting Quantum Interference Device

TFA: Trifluoroacetate

YBCO: Yttrium Barium Copper Oxide